Environmental Science and Pollution Research (2020) 27:607–621
https://doi.org/10.1007/s11356-019-06738-y

RESEARCH ARTICLE

Assessment of soil erosion risk and its response to climate change in the mid-Yarlung Tsangpo River region

Li Wang [1,2] · Fan Zhang [1,2,3] · Suhua Fu [4] · Xiaonan Shi [1] · Yao Chen [1,2] · Muhammad Dodo Jagirani [1,2] · Chen Zeng [1]

Received: 19 February 2019 / Accepted: 10 October 2019 / Published online: 5 December 2019

Abstract

Soil erosion is sensitive to climate change, especially in high mountain areas. The Tibetan Plateau has experienced dramatic land surface environment changes under the impact of climate change during the last decades. In this study, we focused on the mid-Yarlung Tsangpo River (MYZ River) located in the southern part of the Tibetan Plateau. The revised universal soil loss equation (RUSLE) was applied to assess soil erosion risk. To increase its applicability to high mountain areas with longer periods of snowfall, snowmelt runoff erosivity was considered in addition to rainfall erosivity. Results revealed that soil erosion of the MYZ River region was of a moderate grade with an average soil erosion rate of 29.1 t ha^{-1} $year^{-1}$ and most serious erosion in wet and cold years. Soil erosion rate in the MYZ River region showed a decreasing trend of − 1.14% $year^{-1}$ due to the precipitation, temperature, and vegetation changes from 2001 to 2015, with decreasing precipitation being the most important factor. Increasing precipitation and temperature would lead to increasing soil erosion risk in ~ 2050 based on the Coupled Model Intercomparison Project (CMIP5) and RUSLE models. It is clear that soil erosion in high mountain areas greatly depends on climate state and attentions should be paid to address soil erosion problem in the future.

Keywords MYZ River region · Soil erosion · RUSLE · Climatic impacts · Erosion prediction

Introduction

Soil erosion is a worldwide issue that may lead to a number of problems, such as degraded soil productivity, poor water quality, decreased reservoir storage capacity, and disturbance of aquatic life (Zhang and Huang 2015; Lal 2003; Park et al. 2011; Zhang et al. 2015). Thus, quantifying soil erosion is important for the construction of regional ecological environments. In high mountain regions, soil erosion is particularly susceptible to the impacts of changing climate, and research can provide a valuable understanding of hydrological and ecological responses to climate change (IGBP 1996).

It is difficult to get soil erosion measurement data at large scales and soil erosion models have become indispensable tools for assessing the response of soil erosion to climate (Lal 1998; Toy et al. 2002). Previous studies have shown that the climate change is expected to impact the extent, magnitude, and frequency of soil erosion in various ways (Pruski and Nearing 2002). Studies in respect of climate change impacts on soil erosion have been reported over the world, such as in the USA (Parajuli et al. 2016), China (Zhang et al. 2009), the UK (Coulthard et al. 2012), Germany (Routschek et al. 2014), Spain (Bangash et al. 2013), and Portugal (Serpa et al. 2015).

The critical impact of climate change on soil erosion is the change in the erosive power of rainfall (SWCS 2003; Tang et al. 2015), while the rising temperature would influence soil erosion through changes in vegetation cover and soil moisture (Nearing et al. 2004). Study in Germany found that climate change would lead to a significant increase of soil loss by 2050 and a partial decrease by 2100 due to the increasing

Responsible editor: Philippe Garrigues

✉ Fan Zhang
zhangfan@itpcas.ac.cn

[1] Key Laboratory of Tibetan Environment Changes and Land Surface Processes, Institute of Tibetan Plateau Research, Chinese Academy of Sciences, Beijing, China

[2] University of Chinese Academy of Sciences, Beijing, China

[3] CAS Center for Excellence in Tibetan Plateau Earth Sciences, Beijing, China

[4] State Key Laboratory of Earth Surface Processes and Resource Ecology, School of Geography, Beijing Normal University, Beijing, China

trend of extreme rainfall events and the decline of precipitation amount, respectively (Routschek et al. 2014). It is found that the driving force of soil erosion and sediment yields increased from 1961 to 2012 due to the increasing precipitation in the Source Region of the Three Rivers (Wang et al. 2017). Wu et al. (2018) found that soil erosion tended to increase in years observed with high precipitation and in years observed with cold temperature but sufficient precipitation in the northeast of China.

The Tibetan Plateau, also known as "the Third Pole," is one of the most fragile environmental zones in Asia and is vulnerable to soil erosion (Zheng 2003). Major rivers originating from the Tibetan Plateau support billions of people in the surrounding areas and also generate ~ 25% of the global sediment load to nearby oceans (Bandyopadhyay et al. 1997; Immerzeel et al. 2010). Meanwhile, the Tibetan Plateau has experienced severe degradation to its ecosystem due to global and regional climate change (Baumann et al. 2009). Attention should be paid to the soil erosion risk on the Tibetan Plateau to cope with its impacts on hydrological processes and its ecosystem as a result of climate change.

The Yarlung Tsangpo River flows from west to east across the southern region of the Tibetan Plateau, and its midstream serves as the political, economic, and cultural center in Tibet, which has a developed economy and large population (Shi et al. 2018). The assessment of soil erosion risk and studying the influence of climate change on soil erosion along the mid-Yarlung Tsangpo River (MYZ River) would be helpful for understanding soil erosion under climate change scenarios in the Tibetan Plateau. Soil erosion is a phenomenon derived from the denudation and transportation of soil particles and is greatly intensified by human activities, such as excessive deforestation and the conversion of grassland or forests to farmland or infrastructure construction. Erosion is a complicated process influenced by the climate condition, soil properties, topographical factors, land cover, and the interactions between these factors (Ganasri and Ramesh 2016). Major terrain characteristics such as topography, slope, and length play an important role in runoff mechanisms. Steeper slopes lead to higher runoff velocity and, accordingly, more soil erosion. Climate conditions, such as long drought periods followed by heavy rainfall, combined with inappropriate land cover patterns and land use, also cause soil erosion (Renschler et al. 1999). Moreover, the fundamental characteristics of soil can help determine whether the soil is prone to erosion, to some degree. Therefore, effective soil erosion modeling can provide reliable information about the current erosion status and its predicted trends and provide a scenario analysis (Ganasri and Ramesh 2016).

Quantitative models have been developed to calculate soil erosion (Nearing et al. 2005). These models are classified as physically based and empirical types. The empirical models are considered to be a "gray-box" type of model and select the critical factors related to erosion and, thus, predict the amount of soil erosion with observed/calculated materials from the field and laboratory (Park et al. 2011). Physically based models are considered to be a "white-box" type, which represent the soil erosion mechanisms (Ganasri and Ramesh 2016). Well-known physically based models include the European Soil Erosion Model (EROSEM) (Morgan et al. 1998; Khaleghpanah et al. 2016), Soil and Water Assessment Tool (SWAT) (Neitsch et al. 2009; Arnold et al. 2012; Ma et al. 2019), and Water Erosion Prediction Model (WEPP) (Foster and Lane 1987; Nearing et al. 1989, 1990; Laflen et al. 1991; Flanagan and Nearing 1995; Brooks et al. 2016). Each model has its own characteristics. Namely, EROSEM simulates soil loss with a time step of 1 min and is applicable to watersheds with a small slope, while SWAT, which is also watershed-based, is a continuous and daily time-step model simulating water, sediment, nutrients, and chemicals. With respect to WEPP, it is a process model that describes the temporal and spatial distributions of soil erosion and sediment yield from hillslopes and croplands to a watershed.

Major empirical models include universal soil loss equation (USLE) (Tanyaş et al. 2015; Wischmeier and Smith 1978; Vieira et al. 2018), Morgan and Finney methods (Morgan et al. 1984; Hosseini et al. 2018), and the Pacific Southwest Interagency Committee models (PSIAC 1968; Daneshvar and Bagherzadeh 2012). Among these models, USLE is the most important and widely used. The USLE was established by Wischmeier and Smith (1978) and was developed based on thousands of experiments conducted by the Soil Conservation Service and the Agricultural Research Service in 37 US states. With the accumulation of data and increased understanding of soil erosion, the revised universal soil loss equation (RUSLE) was developed to improve the applicability of the model (Meyer 1984; Yoder and Lown 1995; Renard et al. 1997; Foster et al. 2003), which had modifications for slope length, slope factors, and climate factors, as well as a new method for computing vegetation cover factors. The USLE/RUSLE can predict potential erosion cell-by-cell, which is useful for identifying spatial patterns of soil loss in a large area (Shinde et al. 2010). The model has been applied on a watershed scale (Onori et al. 2006; Zhou et al. 2008; Jiang et al. 2015), regional scale (Park et al. 2011; Xu et al. 2013), and national or continental scale (Briggs et al. 1992; Van der Knijff et al. 2000). Due to its simple structure, the model is convenient for calculating soil loss and is also less data-demanding.

Many variables of soil erosion models have a profound difference in temporal and spatial distribution; therefore, new techniques are needed to account for the variability. Moreover, remote sensing has an advantage over conventional methods in obtaining massive and dynamic environmental information quickly (Gitelson et al. 1996). Thus, the application of remote sensing efficiently estimates soil erosion and spatial distribution, with reliability, accuracy, and at a

reasonable cost over large regions (Millward and Mersey 1999; Wang et al. 2003; Gitas et al. 2009; Xu et al. 2009; Schmidt et al. 2018).

The objective of this study is to assess the current erosion conditions, quantify the spatial distribution of soil erosion, and predict the trend of erosion under future climate change conditions in the MYZ River region using the RUSLE model. Doing so will provide essential information for regional soil conservation and improve the understanding of soil erosion in high mountain areas in the face of climate change.

Material and methods

Study area

The MYZ River region also includes the Nyangqu and Lhasa river regions. It is located around 87° 04′ E~92° 37′ E and 28° 16′ N~30° 30′ N. The region covers an area of 67.7 thousand km^2 with an altitude ranging from 3351 m above sea level (asl) to 6932 m asl. The MYZ River region stretches from Xietongmen County, located in the Shigatse District in the west, to Sangri County and Maizhokunggar County, located in the east. From north to south, it lies between the Himalayas and the Gangdise and Nyan ranges of the Tanggula Mountains. The MYZ River region is comprised of 18 counties (cities, districts) and a third of the population is located in the political, economic, and cultural center of Tibet.

Data employed

A digital elevation model (DEM) was applied to identify the influence of the terrain on soil erosion. MODerate Resolution Imaging Spectroradiometer (MODIS), Land Cover Product (MCD12Q1), and Vegetation Indices (MOD13A3) were used to evaluate the impact of soil preservation practices and vegetation conditions on soil erosion. The China Meteorological Forcing Dataset (CMFD) provided precipitation and temperature data for estimating the climate's effect on erosion (Chen et al. 2011), while the China soil map-based Harmonized World Soil Database (HWSD) provided data on soil properties related to soil loss (Table 1). Combined with the topography of the MYZ River region, temperature in high altitude areas was relatively low (Fig. 1). Precipitation and normalized difference vegetation index (NDVI) (Didan 2015) in the east was higher than the west (Fig. 2). The main land use and soil type were comprised of grassland and leptosols, respectively.

Revised universal soil loss equation

In this study, the RUSLE was applied and is described as follows:

$$A = R \times K \times \mathrm{LS} \times C \times P \tag{1}$$

where A is the estimated annual mean soil erosion rate (Mg ha^{-1} year^{-1}), R is the rainfall runoff erosivity factor (MJ mm ha^{-1} h^{-1} year^{-1}), K is the soil erodibility factor (t ha h ha^{-1} MJ^{-1} mm^{-1}), LS is the length of the slope and steepness factor, C is the cover management factor, and P is the support practice factor.

Rainfall runoff erosivity factor

Because R reflects the impact of rainfall and snowmelt, and the associated runoff impact on soil loss (Bissonnais et al. 2005; Chatterjee et al. 2014), in areas with long snowfall, the snowmelt runoff erosivity should be considered (Jiao et al. 2009; Wu et al. 2018). Thus, the rainfall runoff erosivity was calculated as follows:

$$R = R_\mathrm{r} + R_\mathrm{s} \tag{2}$$

where R_r is the rainfall erosivity (MJ mm ha^{-1} h^{-1} year^{-1}) and R_s is the snowmelt runoff erosivity (MJ mm ha^{-1} h^{-1} year^{-1}).

Based on the rainfall and snowfall separation method proposed by Ding et al. (2014), the form of precipitation (i.e., rainfall or snowfall) from May to October was identified as rainfall in this study area. As a result, the 12 months in a year were divided into rainfall periods (May to October) and snowfall periods (November to April). The R_r was calculated based on daily rainfall by the following equation (Zhang et al. 2002; Zhang and Fu 2003; Wu et al. 2018):

$$R_\mathrm{ri} = \alpha \sum_{j=1}^{K} \left(P_j\right)^{\beta} \tag{3}$$

where R_ri is the ith half month rainfall erosivity of the year (MJ mm ha^{-1} h^{-1} year^{-1}), K is the number of days within the corresponding half month, and P_j is the erosive rainfall (daily rainfall higher than 12 mm). The parameters α and β were calculated using the following equations:

$$\beta = 0.8363 + \frac{18.144}{P_\mathrm{d12}} + \frac{24.455}{P_\mathrm{y12}} \tag{4}$$

$$\alpha = 21.586\beta^{-7.1891} \tag{5}$$

where P_d12 is the daily average rainfall of the days with daily rainfall higher than 12 mm during the rainfall period, and P_y12 is the annual average rainfall of the days with daily rainfall higher than 12 mm.

The snowmelt runoff erosivity without gully erosion caused by snowmelt runoff can be described as follows:

$$R_\mathrm{s} = \frac{A_\mathrm{s}}{K_\mathrm{s}\mathrm{LS}C_\mathrm{s}P} \tag{6}$$

where A_s is the soil erosion rate of snowfall period (Mg ha^{-1} year^{-1}), K_s is soil erodibility of snowfall period (t ha h ha^{-1} MJ^{-1} mm^{-1}), and C_s is cover management factor of snowfall period.

Table 1 Dataset collected to estimate soil loss

Dataset	Content	Resolution	Source
Precipitation	Precipitation of CMFD from 2001 to 2015	Daily, 10 km	http://westdc.westgis.ac.cn
Temperature	Temperature of CMFD from 2001 to 2015	Daily, 10 km	http://westdc.westgis.ac.cn
Soil	Topsoil organic carbon, subsoil clay fraction, sand fraction, and silt fraction from HWSD	1 km	http://westdc.westgis.ac.cn
DEM	ASTER GDEM	30 m	https://search.earthdata.nasa.gov
NDVI	MODIS/Terra Vegetation Indices product	Monthly, 1 km	https://search.earthdata.nasa.gov
Land use	MODIS Land Cover Type product	Annual, 1 km	https://search.earthdata.nasa.gov

According to the definition of sediment delivery ratio, the soil erosion rate during the snowfall period can be expressed as

$$A_s = \frac{Y_s}{D_s} \tag{7}$$

where Y_s is riverine sediment load (Mg ha^{-1} year^{-1}) and D_s is sediment delivery ratio of snowfall period.

Similarly, the rainfall erosivity and soil erosion rate during the rainfall period can be described by the following equations:

$$R_r = \frac{A_r}{K_r L S C_r P} \tag{8}$$

$$A_r = \frac{Y_r}{D_r} \tag{9}$$

where A_r is the soil erosion rate of rainfall period (Mg ha^{-1} year^{-1}), K_r is the soil erodibility of rainfall period (t ha h ha^{-1} MJ^{-1} mm^{-1}), C_r is the cover management factor of rainfall period, Y_r is the riverine sediment load, and D_r is the sediment delivery ratio of rainfall period.

Assuming that the sediment delivery ratio and the C factor are equal in their periods of snowfall and rainfall (Jiao et al. 2009), the snowmelt runoff erosivity can be deduced as

$$R_s = \frac{Y_s K_r}{Y_r K_s} R_r \tag{10}$$

Using the sediment yield data at three stations in and around the study area that are available during the rainfall and snowfall period from 2007 to 2009 (Table 2), the snowmelt runoff erosivity of these 3 years in the three sub-basins were estimated using Eqs. (3–10). Based on the high

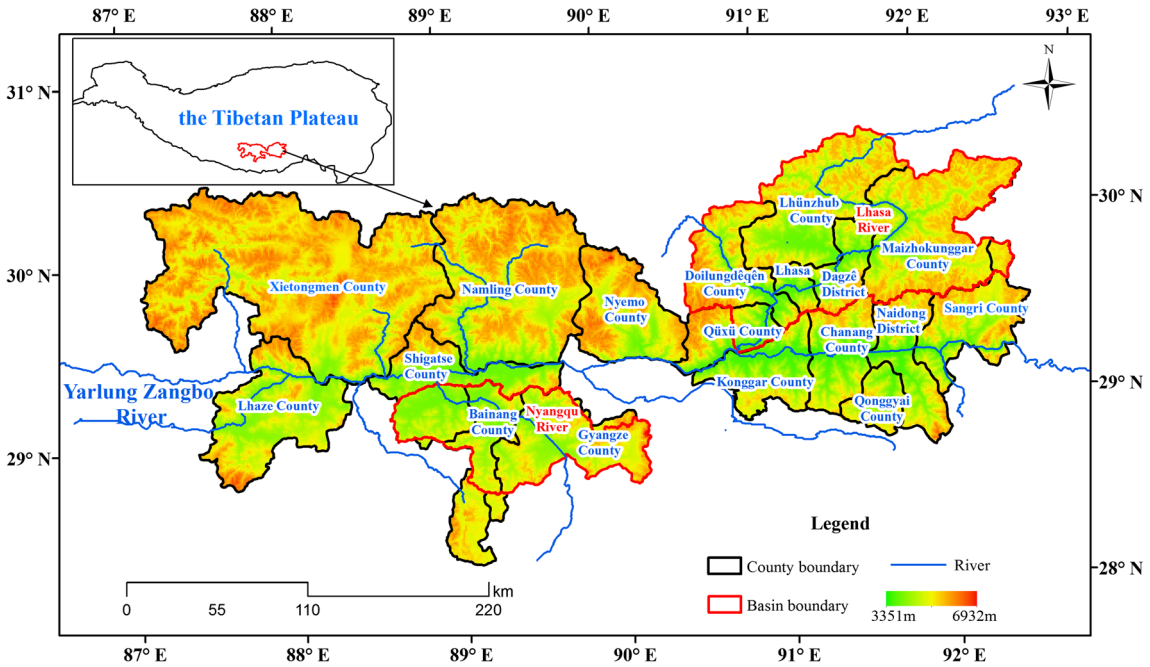

Fig. 1 Location and topography of the MYZ River region in the Tibetan Plateau

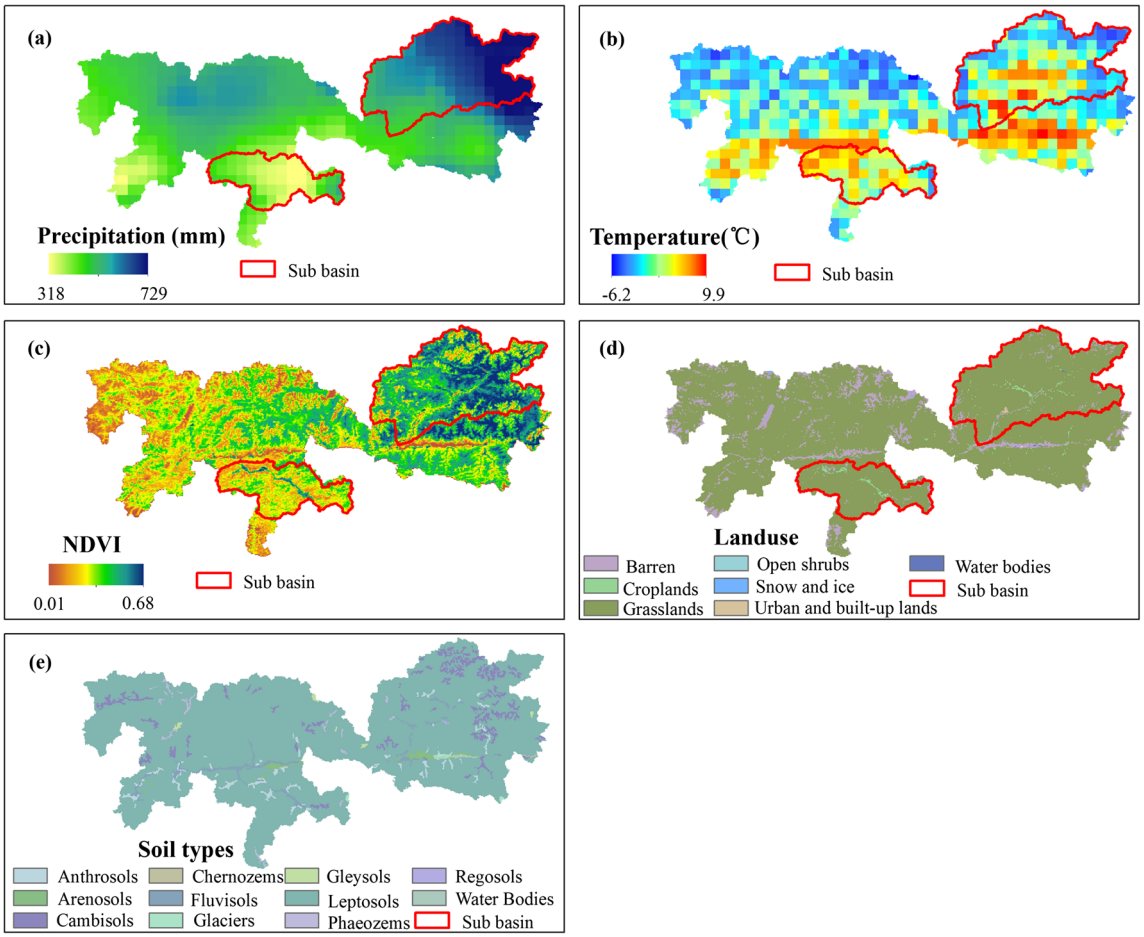

Fig. 2 Spatial distribution of **a** annual precipitation (Chen et al. 2011), **b** mean air temperature (Chen et al. 2011), **c** NDVI (Didan 2015), **d** land use (https://search.earthdata.nasa.gov), and **e** soil types (http://westdc.westgis.ac.cn)

correlation between the calculated snowmelt runoff erosivity and the corresponding precipitation (R^2 = 0.833), the regression relationship between the two variables was established, i.e., Eq. (11) (Fig. 3), and used to calculate the snowmelt runoff erosivity of other years.

$$R_s = 6.99 + 4.17P_s \quad R^2 = 0.833 \tag{11}$$

where P_s is the amount of snowfall during snowfall period.

Soil erodibility factor

The soil erodibility factor (K) indicates the susceptibility of soil to erosion under unit plot conditions (Renard et al. 2011).

Table 2 Basic information of the hydrological stations of the Yarlung Tsangpo River

Station	Longitude	Latitude	River	Time period
Poindo	91.35	30.1	Lasha	2007–2009
Shigatse	88.9	29.28	Nyangchu	2007–2009
Yangcun	91.88	29.29	Yarlung Tsangpo	2007–2009

Generally, K values for clay and sandy soils are low due to the resistance to detachment and high infiltration rates, respectively. The K values of silt soils are the highest, as the soil crusts readily generating high runoff and massive sediment. Soil particle size and soil organic carbon are used to calculate K value with the following formulas described by Sharpley and Williams (1990):

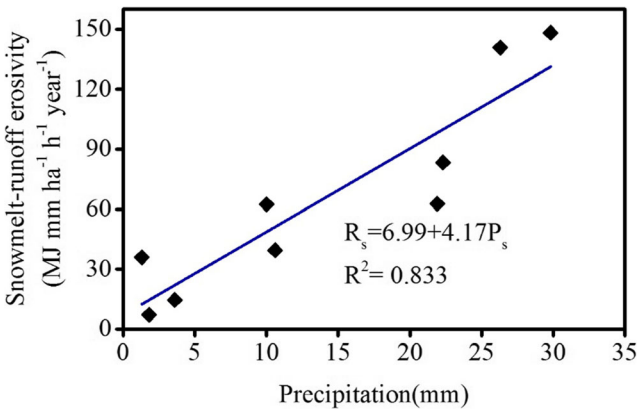

Fig. 3 The relationship between the snowmelt runoff erosivity and precipitation during the snowfall period

$$K = 0.1317 \times f_{\text{csand}} \cdot f_{\text{cl–si}} \cdot f_{\text{orgc}} \cdot f_{\text{hisand}} \tag{12}$$

$$f_{\text{csand}} = 0.2 + 0.3\exp\left[-0.0256 \cdot m_s \cdot \left(1-\frac{m_{\text{silt}}}{100}\right)\right] \tag{13}$$

$$f_{\text{cl–si}} = \left(\frac{m_{\text{silt}}}{m_{\text{cl}} + m_{\text{silt}}}\right)^{0.3} \tag{14}$$

$$f_{\text{csand}} = 1-\frac{0.25\text{orgC}}{\text{orgC} + \exp\left(3.72-2.95\text{orgC}\right)} \tag{15}$$

$$f_{\text{hisand}} = 1-\frac{0.7\left(1-\frac{m_s}{100}\right)}{\left(1-\frac{m_s}{100}\right) + \exp\left(-5.51 + 22.9\left(1-\frac{m_s}{100}\right)\right)} \tag{16}$$

where m_{silt}, m_c, and m_s are silt fractions (0.002–0.05-mm-diameter particles), clay fractions (< 0.002-mm-diameter particles), and sand fractions (0.05–2.00-mm-diameter particles) and orgC is topsoil organic carbon content (%).

These K values vary across the year and are influenced by temperature. The estimated values calculated by the formulas above are assumed to be the base values for "frost free" period. According to RUSLE2 developed by the USDA-Agricultural Research Service (2008), K values decrease exponentially as a function of temperature when the temperature is below − 1.1 °C and are approximately 0 at a temperature of − 9.4 °C. There are various terrain units in the region, including valley plains, and mountain plateaus with large altitude differences. As temperature varies with altitude, the spatial difference should be taken into consideration when calculating the temperature effect on the K factor. The difference is calculated as

$$K_t = \begin{cases} K & t \geq -1.1°C \\ K \times \exp(t) & t < -1.1°C \end{cases} \tag{17}$$

where K is the value estimated by Eq. (12), t is the temperature (°C), and K_t is the soil erodibility influenced by temperature.

Slope length and steepness factor

The geographic factor (LS) mainly reflects the impact of topography on soil erosion (Park et al. 2011). Generally, greater LS factors generate higher overflow velocity and correspondingly larger erosion (Ozsoy et al. 2012). The slope length is calculated from where water begins to flow to where sedimentation starts. The steepness is the average slope gradient of the terrain and is conveyed as a percentage of the vertical height over a horizontal distance. The basic input for LS calculation is from the DEM dataset (Park et al. 2011). The L factor of LS was calculated using the following formula (Foster and Wischmeier 1974; Fu et al. 2015):

$$L_i = \frac{\left(\lambda_{\text{out}}^{m+1} - \lambda_{\text{in}}^{m+1}\right)}{\left(\left(\lambda_{\text{out}} - \lambda_{\text{in}}\right)22.13^m\right)} \tag{18}$$

where L_i is the slope length factor of the i grid, λ_{out} and λ_{in} are the slope length of the outlet and inlet, respectively (m), and m is the exponent of the slope length. The exponent can be calculated using Eq. (10) as follows:

$$m = \begin{cases} 0.2 & \theta < 0.5° \\ 0.3 & 0.5° \leq \theta < 1.5° \\ 0.4 & 1.5° \leq \theta < 3° \\ 0.5 & \theta \geq 3° \end{cases} \tag{19}$$

where θ is the slope angle.

The S factor was estimated based on the following formula (Mccool et al. 1987; Liu et al. 1994):

$$S = \begin{cases} 10.8\sin\theta + 0.03 & \theta < 5° \\ 16.8\sin\theta - 0.5 & 5° \leq \theta < 10° \\ 21.91\sin\theta - 0.96 & \theta \geq 10° \end{cases} \tag{20}$$

Cover management factor

The cover management factor (C) represents the extent to which vegetation reduces soil loss. The value often depends on surface roughness, soil moisture, prior land use, surface cover, and canopy cover (Renard et al. 1997). It is also difficult to estimate the variables for a large area of non-agricultural land (Zhou et al. 2008). To reflect the spatial variability of vegetation cover, satellite images were used to establish the relationship between the C factor and remote sensing information (band composition or vegetation index) (Van der Knijff et al. 2000; Zhou et al. 2008). The MODIS NDVI data were used to calculate the C factor through the following equation (Van Leeuwen and Sammons 2004):

$$C = \exp\left(-2.5 \times \frac{\text{NDVI}}{1-\text{NDVI}}\right) \tag{21}$$

where C is the value of cover management factor. The NDVI data reflect the information of green vegetation, but the images cannot detect the protection of surface litter to the soil, which may lead to the overestimation of the C factor for the snowfall period (Lei and Wen 2008). Therefore, the averaged C value of the rainfall period was used to estimate annual soil erosion rate (Jiao et al. 2009).

Support practice factor

The support practice factor is defined as the ratio of soil loss with upward and downward slope tillage under the soil preservation policy (Renard et al. 1997). The P factor value is usually estimated by the types of land cover and was determined by previous studies (i.e., 1 for forest, grassland, shrub,

or bare land; 0.4 for cropland; and 0 for a body of water, snow/ice, or built-up areas) (Jain et al. 2001; Naqvi et al. 2013).

Contribution of various factors to soil erosion change Wang et al. (2015) drew information from Kaya identity and applied it to identify the contributions of various factors influencing sediment load. In the formulation, the proportional change rate $r(X)$ of a quantity $X(t)$ was defined as:

$$r(X) = X^{-1}\frac{dX}{dt} \tag{22}$$

where dx/dt is the derivative of X and can be expressed as X'.

The formula is used as a reference to calculate the contribution of the R, K, LS, C, and P factors to the relative change of soil erosion rate in the MYZ River region. Taking the derivative of both sides, E (1) can be converted as follows:

$$\frac{A'}{A} = \frac{R'}{R} + \frac{K'}{K} + \frac{C'}{C} + \frac{\mathrm{LS}'}{\mathrm{LS}} + \frac{P'}{P} \tag{23}$$

Consequently, the changing rate of soil erosion can be calculated based on the changing rate of its influential factors as

$$r(A) = r(R) + r(K) + r(\mathrm{LS}) + r(C) + r(P) \tag{24}$$

where r is the proportional change rate. With this, the contribution of R, K, C, LS, and P factor to the change of soil erosion could be evaluated.

Prediction of future soil erosion

The impacts of climate change and major contributing factors, such as the effects of precipitation and temperature on soil erosion, have been reported (Li and Fang 2016). The intensity, amount, and spatiotemporal distribution of precipitation affect soil erosion directly, while the rise in temperature affects soil erosion indirectly (Li and Fang 2016; Teng et al. 2018). Global climate models (GCMs) are used for understanding the present climate and forecasting future climate change conditions. These GCMs take into account various systems, namely, atmospheric, terrestrial, and oceanic systems. However, GCMs are unable to assess the climate effects on specific sites reliably due to their coarse spatial resolution (Hulme et al. 1993; Zhang and Nearing 2005). Downscaling methods have been developed to resolve this issue. There are two main downscaling methods: dynamic downscaling and statistical downscaling. Due to the intensive computation required in the dynamic downscaling approach, the statistical downscaling approach is widely used instead and is easy to establish, has efficient computation, and has good transferability.

The Geophysical Fluid Dynamics Laboratory (GFDL) climate model was used to obtain future climatic factors for ~ 2050. Three representative concentration pathways (RCPs), RCP 2.6, RCP 4.5, and RCP 8.5, were applied to derive future estimates of RUSLE factors. RCP 2.6, RCP 4.5, and RCP 8.5 signify radiative forcing values of 2100 versus pre-industrial values (+ 2.6, + 4.5, and + 8.5 W/m^2, respectively). The delta method was adopted to produce local scale meteorological series (Hay et al. 2000). The final calculation of soil erosion for ~ 2050 was derived with predicted R, K, C, LS, and P factors following Eq. (1). In particular, most of the land cover of the MYZ River region was grassland and the land use type barely changed, so the mean P factor from 2001 to 2015 was used for predictions of the near future. The LS factor was dependent on topography and was also assumed to be the same in the near future. Daily precipitation and temperature for ~ 2050 will be obtained from the climate model. Then these data would be used to estimate the R and K factors based on the corresponding equation above. In the MYZ River region, monthly NDVI showed a notable positive correlation with monthly precipitation during 2001–2015 (NDVI = 0.0016 P + 0.158, R^2 = 0.758). Therefore, NDVI was predicted based on precipitation, and then the predicted NDVI was used to estimate the C factor.

Results

Soil erosion state

The mean annual R factor of the MYZ River region was 867.6 MJ mm ha^{-1} h^{-1} year^{-1} from 2001 to 2015, which was consistent with the value of Teng et al. (2018) (Fig. 4a). The R factor was positively correlated with the amount of precipitation. The average precipitation of the MYZ River region, Lhasa River basin, and Nyangqu River basin were 477.0 mm, 564.2 mm, and 380.2 mm, respectively. As a result, the lowest values of the R factor were observed in the Nyangqu River basin while the highest R values were found in the Lhasa River region (Fig. 4a).

Lower K values were found in the northwest part of the study area, indicating the soils in that area are not easily detached and transported. The average K value without consideration of the influence of temperature was 0.034 t ha h ha^{-1} MJ^{-1} mm^{-1}, which is similar to previous studies (Liu et al. 2014; Teng et al. 2018). Taking the effect of temperature into consideration, the mean value of K was reduced to 0.022 t ha h ha^{-1} MJ^{-1} mm^{-1}, indicating that annual mean soil erodibility could be overestimated omitting the effect of soil freezing (Fig. 4b).

The mean value of the C factor was 0.28, which was consistent with previous studies (Fu et al. 2005; Du et al. 2016); C values were simply assigned based on land use type (Teng et al. 2018). In the MYZ River region, grassland is the main land use type and the C value calculation represented the

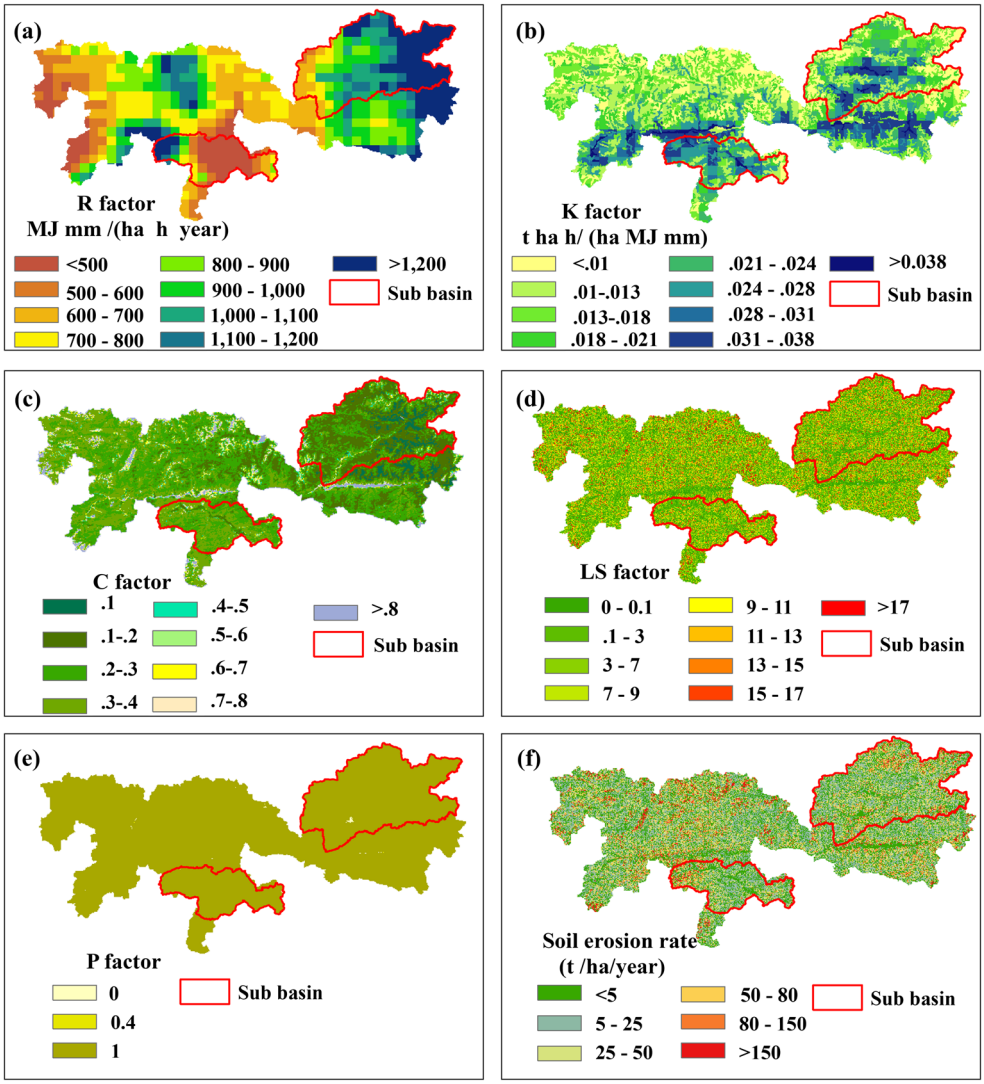

Fig. 4 Mean values at a 1-km resolution **a** rainfall runoff erosivity, *R* factor; **b** soil erodibility, *K* factor; **c** slope and steepness, LS factor; **d** cover management, *C* factor; **e** soil preservation, *P* factor; and **f** soil erosion grades of MYZ River region from 2001 to 2015

spatial variation of slightly decreasing pattern from east to west, indicating denser vegetation cover in the eastern part of the region compared to the west (Fig. 4c).

The mean value of the MYZ River region was 5.10 with a standard deviation of 5.13, illustrating that LS values were unevenly distributed (Fig. 4d). In the MYZ River region, human activities are limited due to the harsh climate and extreme terrain. Therefore, the value of the *P* factor was close to 1 due to a large area of grassland lacking effective conservation practices (Fig. 4e).

The soil erosion rate in the western part of the region tended to be higher than the east when the *R* factor was at the same level and the *K* factor was relatively lower. This may be due to better vegetation conditions in the east, which led to lower *C* values and correspondingly lower soil erosion rates (Fig. 4f).

The average annual soil erosion rate was 29.1 t ha^{-1} $year^{-1}$, belonging to the moderate grade, and the annual soil loss was ~ 196.8 million tons, which is at the same level with the results of Teng et al. (2018). According to the statistical results, 36.38% of the MYZ River region was under a slight erosion grade, 27.66% was under a light erosion grade, and 18.29% was under a moderate erosion grade (Table 3). The severe to extreme erosion grades accounted for 17.67% of the study area. When taking the annual soil loss into consideration, ~ 63.16% of the total soil loss was derived from severe and extreme erosion grades, while the corresponding erosion area only occupied a small proportion of the MYZ River region. The rest of the soil loss was mainly due to light and moderate erosion grades. Soil loss from slight erosion grade was only 0.45%, which was quite low compared to larger erosion areas.

Soil erosion characteristics

The study period of 15 years was separated into three categories using the *k*-means clustering method based on

Table 3 Statistics of soil erosion grades

Grade	Criterion of erosion rate[a,b]	Area percent (%)	Erosion area (10^5 ha)	Soil loss (10^6t year^{-1})	Soil loss percent (%)
Slight	< 5	36.38	24.63	0.89	0.45
Light	5–25	27.66	18.73	27.46	13.95
Moderate	25–50	18.29	12.38	44.18	22.44
Severe	50–80	8.75	5.92	37.05	18.82
Very severe	80–150	6.24	4.22	44.71	22.71
Extreme	> 150	2.68	1.82	42.59	21.63

[a] SL190-2007 (Ministry of Water Resource of China 2007)

[b] Unit: t ha^{-1} year^{-1}

precipitation and temperature (Wu et al. 2018). Namely, category C1 was characterized by wet and cold years with higher precipitation and lower temperature, category C2 was characterized by dry and hot years with lower precipitation and higher temperature, and category C3 was defined as a normal year with moderate temperature and precipitation. Years with adequate precipitation were often accompanied with lower temperature, while years with lower precipitation tended to have higher temperature.

The average soil erosion rate for C1, C2, and C3 was 40.0, 18.9, and 26.6 t ha^{-1} year^{-1}, respectively (Table 4). The average soil erosion rate in C1 was 50.4% higher than C3, while the average soil erosion rate in C2 was 28.9% lower than C3. Characterized with sufficient precipitation and lower temperature, C1 was the most prone to soil erosion. It can be concluded that precipitation was the dominant factor of soil erosion, although sufficient precipitation with higher rainfall runoff erosivity and lower temperatures were indicative of lower soil erosivity and may have the opposite effect. These results are consistent with Wu et al. (2018), who conducted a study on a freezing-thawing watershed in northeastern China.

Temporal variation of RUSLE factors

The highest rainfall erosivity and snowmelt runoff erosivity were in 2014 (1504.3 MJ mm ha^{-1} h^{-1} year^{-1}) and 2015 (297.6 MJ mm ha^{-1} h^{-1} year^{-1}), respectively. The snowmelt runoff erosivity accounted for only 17.7% of the rainfall runoff erosivity. Compared to rainfall erosivity, the change in snowmelt erosivity was relatively stable. Although the annual precipitation showed a decreasing trend, the precipitation in snowfall period had an increasing trend; accordingly, the snowmelt runoff erosivity showed an increasing trend (Fig. 5a, b).

Although temperature during the rainfall period showed an increasing trend, the change in the *K* factor was relatively small because the temperature was relatively high and its impact on the *K* factor was minimal from May to October (Fig. 5c). Temperature had a decreasing trend during the snowfall period, resulting in a decreasing *K* value, and soil erodibility varied dramatically during snowfall period (Fig. 5d). When the temperature was high in the snowfall period, the soil started thawing earlier and the *K* factor tended to be larger. Soil erodibility was stable during the rainfall period and showed a decreasing trend during the snowfall period. Annual *K* values had a downward trend despite increasing annual mean temperature from 2001 to 2015.

The *C* factor fluctuated from 2001 to 2015, but the change was not dramatic (Fig. 5e). Based on the three categories, the *C* factor was lower in C1 (wet cold years). This indicated reduced soil erosion under better vegetation conditions in years with adequate precipitation.

The study area was mainly covered by grassland, while cropland or built-up areas were scarce due to its high terrain and extreme climate. Thus, the *P* value was close to 1 and remained almost unchanged. The LS factor was also unchanged from 2001 to 2015.

Contribution of various factors to soil erosion change

The soil erosion rate of the MYZ River region showed a decreasing trend with a proportional changing rate of − 1.14% year^{-1} from 2001 to 2015. The main factors contributing to the decreasing soil erosion rate were the *R*, *K*, and *C* factors. Based on the Kaya identity, the contributions of the *R*, *K*, and *C* factors on the decreasing soil erosion rate were 95.8%, 3.9%, and 0.3% year^{-1}, respectively. This indicated that the most important factor influencing soil erosion change was precipitation.

Projected future soil erosion rate of the MYZ River region

The precipitation in ~ 2050 was predicted to increase by 17.9%, 18.8%, and 21.4% under RCP 2.6, RCP 4.5, and RCP 8.5, respectively, when compared to the 2001–2015 period. Temperature was predicted to increase by 0.2 °C, 0.3 °C,

Table 4 Yearly soil erosion characteristics for different categories

Category	Average (t ha^{-1} year^{-1})	Max (t ha^{-1} year^{-1})	Min (t ha^{-1} year^{-1})
C1	40.0	58.0	29.9
C2	18.9	20.2	18.0
C3	26.6	35.7	21.0
All years	29.1	58.0	18.0

and 0.6 °C under RCP 2.6, RCP 4.5, and RCP 8.5, respectively. Based on future precipitation and temperature changes, the *R* factor will increase by 34%, 36%, and 39% under RCP2.6, RCP 4.5, and RCP8.5, respectively, while the *K* factor will increase by 1.8%, 2.3%, and 4.2%, respectively. Under RCP 2.6, RCP 4.5, and RCP 8.5, the *C* factor will decrease by 0.16%, 0.17%, and 0.19%, respectively. The LS and *P* factors were assumed to be unchanged above. As a result, the soil erosion rate under RCP 2.6, RCP 4.5, and RCP 8.5 was predicted to be 39.4, 40.2, and 41.6 t ha^{-1} year^{-1}, respectively.

Discussion

Links between soil erosion and climate change

High mountain areas are sensitive to climate change and the changing climactic conditions may increase the risk of soil loss and land degradation in these areas, like that of the Tibetan Plateau (Wang et al. 2017). The MYZ River region is not only an economic development zone but also has suffered from a great deal of soil loss.

The annual precipitation had a weak decreasing trend in the MYZ River region from 2001 to 2015, and as a result, the *R* factor showed a decreasing trend as well. Although the annual temperature and temperature during the rainfall period had an increasing trend, temperature during the snowfall period had a decreasing trend and a decreasing *K* value. However, in the near future, precipitation and temperature during the rainfall and snowfall periods are predicted to have an increasing trend, causing higher *R* and *K* factors and a corresponding higher soil erosion rate.

Influence of climate change on soil erosion characteristics

According to previous studies, the characteristics of soil erosion are influenced by precipitation and temperature, and precipitation is the most influential factor contributing to soil erosion (Vente and Poesen 2005; Wu et al. 2018; Li and Fang 2016). Pruski and Nearing (2002) found that every 1% change in precipitation may induce a 1.7% change in soil erosion based on sensitivity analyses. Similarly, Lu et al. (2013) investigated eight large Chinese rivers and suggested that each 1% change in precipitation would lead to a 2% change in sediment loads. Higher ranges were reported by Zhang (2007), who founded that a 4–18% increase in precipitation may result in a 31–167% increase in soil loss in the Loess Plateau region of China. In this study, precipitation and temperature were the leading contributing factors with precipitation primarily affecting soil erosion change from 2001 to 2015. Furthermore, it is estimated that every 1% increase in precipitation may induce a 1.8% increase in soil erosion rate in the MYZ region. Although the snowmelt runoff erosivity accounted for 13.6% of the total rainfall runoff erosivity, soil erosion in the snowfall period accounted for only 5.9% of the annual soil erosion from 2001 to 2015. This is likely due to low temperatures during the snowfall period, thus causing soil to freeze and reducing its erodibility.

Uncertainties in soil erosion assessment

An equation for estimating snowmelt runoff erosivity in the snowfall period was established, which was more applicable for high mountain areas. Therefore, the snowmelt runoff erosivity and rainfall erosivity in the MYZ River region were calculated separately. However, it should be noted that the equation used was derived based on the assumption of an equal sediment delivery ratio and *C* factor during the snowfall and rainfall periods. Thus, there may be some deviation from the actual value. Similarly, as reported in a previous study investigating watersheds with a high proportion of snowfall in the Heilongjiang Province, snowmelt runoff erosivity was usually underestimated (Jiao et al. 2009). However, it was still practical for the areas without snowmelt runoff erosion monitoring, especially in high mountain areas, because soil erosion in these areas is difficult to measure and monitor due to the harsh climate conditions. To further improve the accuracy of these calculations, the monitoring of snowmelt runoff erosion needs to be strengthened in the future.

The formulation used to calculate *K* was proposed by USDA-Agricultural Research Service based on the observation data in the USA, introducing uncertainty while applied to other regions. Soil would freeze and thaw with the change of

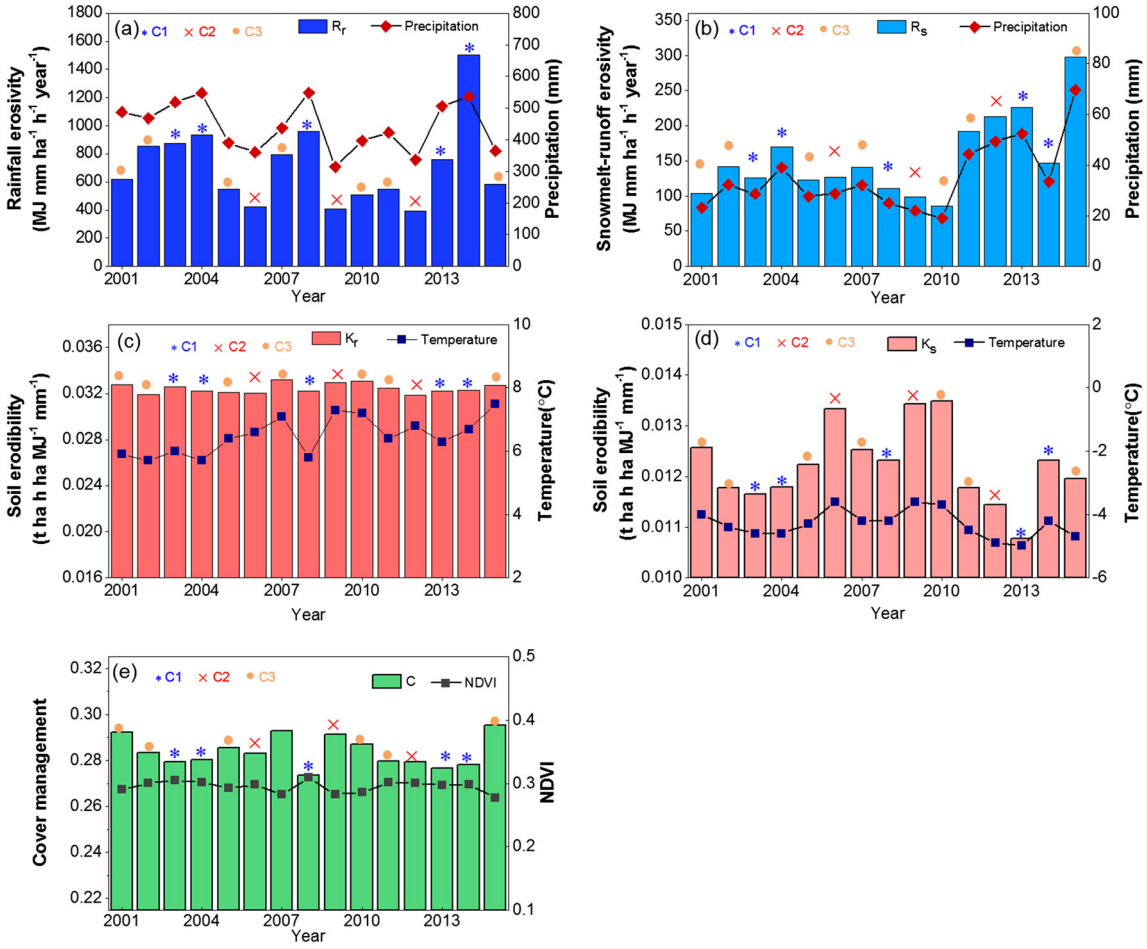

Fig. 5 Temporal variation in **a** rainfall erosivity, **b** snowmelt runoff erosivity, **c** soil erodibility in rainfall period, **d** soil erodibility in snowfall period, and **e** cover management

temperature. Studies show that freezing and thawing mainly influence soil erodibility by changing soil water content (Musa et al. 2016), bulk density (Dagesse 2010), shear strength (Zhou et al. 2017), and agglomerate stability (Sahin et al. 2008). Therefore, future study is suggested to quantify the freezing and thawing effect on soil erodibility and validate the applicability of Eq. (17) to the Tibetan Plateau through the simulation of freezing and thawing environment and indoor soil physical and chemical properties determination.

It should be noted that there were some limitations in this study, especially for the estimation of the *C* factor. Monthly MODIS NDVI data were used to obtain the temporal and spatial distribution of the *C* factor. Generally, NDVI is inversely related to soil erosion. The larger the NDVI value, the smaller the *C* factor value. However, NDVI is easily saturated in areas with high vegetation coverage and is more or less affected by background information, such as soil, resulting in noise in the NDVI data (Wu et al. 2012). Moreover, during the snowfall period, the vegetation factor is easily underestimated as NDVI data reflect the information of green vegetation only, which may lead to an overestimation of the *C* factor. To alleviate this problem, the *C* factor during the snowfall period was assumed to be the same as in the rainfall period. However, realistically, there was likely a difference in the real *C* values between the snowfall and rainfall periods. Additionally, the method used in this study to calculate the *C* factor may induce some uncertainty. To improve the accuracy of *C* factor calculations in future studies, other indexes, such as the Normalized Difference Tillage Index (NDTI) and the Normalized Difference Senescent Vegetation Index (NDSVI), could be taken into consideration aside from the NDVI to explore the effect of surface litter (Wu et al. 2012).

Conclusions

This study investigated soil erosion risk and the climatic impacts in a high mountain region by RUSLE based on essential meteorological data, soil properties, and vegetation conditions from 2001 to 2015 and predicted

conditions in the future. Snowmelt runoff erosivity was estimated based on the precipitation amount during the snowfall period due to lack of onsite monitoring of snowmelt. The influence of temperature, i.e., frozen and thaw, on soil erodibility was also considered. The results revealed that (1) the soil erosion rate of the MYZ River region during 2001–2015 was 29.1 t ha^{-1} $year^{-1}$ and annual soil loss reached 194.4 million tons. Although area of severe to extreme soil erosion was small (~ 17.28%), it caused the largest amount of soil loss with a proportion of 62.59%. (2) Soil erosion rate showed a decreasing trend of − 1.14% $year^{-1}$ due to the precipitation, temperature, and vegetation change from 2001 to 2015. Moreover, the dominant contribution factor is decreasing precipitation because of its great influence on rainfall runoff erosivity. (3) Precipitation was the leading factor contributing to soil erosion. In the three climatic categories identified based on *k*-mean clusters, i.e., wet cold (C1), dry hot (C2), and normal (C3) years, soil erosion rates for C1 was most severe (40.0 t ha^{-1} $year^{-1}$ compared to 18.9 and 26.6 t ha^{-1} $year^{-1}$ for C2 and C3, respectively). Lastly, (4) soil erosion shows an increasing trend in the near future because of the increased precipitation and temperature and corresponding *R* and *K* factors. Specifically, soil erosion rate is predicted to be 39.4, 40.2, and 41.6 t ha^{-1} $year^{-1}$ under RCP 2.6, RCP 4.5, and RCP8.5 in ~ 2050, respectively. The findings of this study clearly demonstrated that soil erosion in high mountain regions has been influenced by climate change. More attention should be paid to soil erosion control in the MYZ River region, and concentrated efforts on the small proportion of area graded with severe to extreme soil erosion would be an efficient way to begin to address these concerns.

Acknowledgments This research was financially supported by the "Second Tibetan Plateau Scientific Expedition and Research Program" (2019QZKK0203) and the "Strategic Priority Research Program" of the Chinese Academy of Sciences (XDA20060202) and the National Natural Science Foundation of China (Grant No. 41771090 and No. 41571274).

Appendix. Rainfall runoff erosivity during snowfall and rainfall period

Based on previous studies, the sediment delivery ratio ranged from 0.02 to 0.98 and largely depended on the watershed scale (Porto et al. 2011; Zhang et al. 2015). The average sediment delivery ratio of the snowfall and rainfall period at the Nuxia station (94° 39′ E, 294 28 N) of the Yarlung Tsangpo River were calculated based on the station data during 2001–2015 to be 0.11 and 0.12, respectively. The box plot (Fig. 6) showed that there is no significant difference between the sediment delivery ratios of the snowfall and rainfall periods at the Nuxia station, supporting our assumption that the sediment delivery ratios are equal in the periods of snowfall and rainfall in the study area.

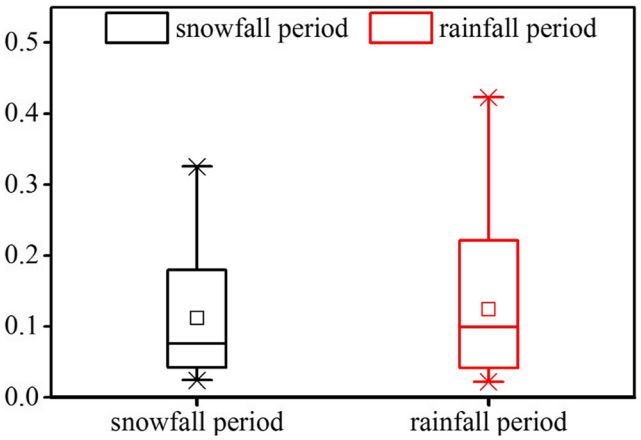

Fig. 6 Box plot of sediment delivery ratio at the Nuxia station during the snowfall and rainfall period

References

Arnold JG, Kiniry JR, Srinivasan R, Williams JR, Haney EB, Neitsch SL (2012) Soil and Water Assessment Tool Theoretical Documentation Input/output Documentation Version 2012

Bandyopadhyay J, Rodda JC, Kattelmann R, Kundzewicz ZW, Kraemer D (1997) Highland water—a resource of global significance. In: Messerli B, Ives JD (eds) Mountains of the world: a global priority. Parthenon, Carnforth, pp 131–155

Bangash RF, Passuello A, Sanchez-Canales M, Terrado M, López A, Elorza FJ, Ziv G, Acuña V, Schuhmacher M (2013) Ecosystem services in Mediterranean river basin: climate change impact on water provisioning and erosion control. Sci Total Environ 458–460:246–255

Baumann F, He JS, Schmidt K, Kuhn P, Scholten T (2009) Pedogenesis, permafrost, and soil moisture as controlling factors for soil nitrogen and carbon contents across the Tibetan Plateau. Glob Chang Biol 15(12):3001–3017

Bissonnais Y, Nichols MH, Nunes JP, Renschler CS, Souche're V, van Oost K (2005) Modeling response of soil erosion and runoff to changes in precipitation and cover. Catena 61:131–154

Briggs D, Giordano A, Cornaert M, Peter D, Maes J (1992) CORINE soil erosion risk and important land resources in the southern regions of the European Community. Commission of the European Communities Publication EUR 13233

Brooks ES, Dobre M, Elliot WJ, Wu JQ, Boll J (2016) Watershed-scale evaluation of the water erosion prediction project (WEPP) model in the Lake Tahoe basin. J Hydrol 533:389–402

Chatterjee S, Krishna AP, Sharma AP (2014) Geospatial assessment of soil erosion vulnerability at watershed level in some sections of the upper Subarnarekha River basin, Jharkhand, India. Environ Earth Sci 71(1):357–374

Chen Y, Yang K, Jie H, Qin J, Shi J, Du J, He Q (2011) Improving land surface temperature modeling for dry land of china. J Geophys Res Atmos 116(D20)

Coulthard TJ, Ramirez J, Fowler HJ, Glenis V (2012) Using the UKCP09 probabilistic scenarios to model the amplified impact of climate change on drainage basin sediment yield. Hydrol Earth Syst Sci 16(11):4401–4416

Dagesse DF (2010) Freezing-induced bulk soil volume changes. Can J Soil Sci 90(3):389–401

Daneshvar MRM, Bagherzadeh A (2012) Evaluation of sediment yield in PSIAC and MPSIAC models by using GIS at Toroq watershed, northeast of Iran. Front Earth Sci 6(1):83–94

Didan K (2015) MOD13A3 MODIS/Terra Vegetation Indices Monthly L3 Global 1 km SIN Grid V006 [Data set]. NASA EOSDIS LP DAAC. https://doi.org/10.5067/MODIS/MOD13A3.006

Ding B, Yang K, Qin J, Wang L, Chen Y, He X (2014) The dependence of precipitation types on surface elevation and meteorological conditions and its parameterization. J Hydrol 513(11):154–163

Du HQ, Dou ST, Deng XH, Xue X, Wang T (2016) Assessment of wind and water erosion risk in the watershed of the Ningxia-Inner Mongolia Reach of the Yellow River, China. Ecol Indic 67:117–131

Flanagan DC, Nearing MA (1995) USDA-Water Erosion Prediction Project (WEPP) hillslope profile and watershed model documentation

Fu BJ, Zhao WW, Chen LD, Zhang QJ, Lu YH, Gulinck H et al (2005) Assessment of soil erosion at large watershed scale using RUSLE and GIS: a case study in the Loess Plateau of China. Land Degrad Dev 16(1):73–85

Foster GR, Lane LJ (1987) User requirements: USDA-water erosion prediction project (WEPP). NSERL report NO.1.West Lafayette: USDA-Agricultural Research Service.

Foster GR, Wischmeier WH (1974) Evaluating irregular slopes for soil loss prediction. Trans Am Soc Agric Eng 17(2):305–309

Foster GR, Toy TE, Renard KG (2003) Comparison of the USLE, RUSLE1.06 and RUSLE2 for application to highly disturbed lands. In: Renard KG, Mc. Ilroy SA, Gburek WJ, Cranfield HE, Scott RL (eds) First Interagency Conference on Research in Watersheds, October 27–30, 2003. US Department of Agriculture

Fu S, Liu B, Zhou G, Sun Z, Zhu X (2015) Calculation tool of topographic factors. Sci Soil Water Conserv 13(5):105–110 (in Chinese)

Ganasri BP, Ramesh H (2016) Assessment of soil erosion by RUSLE model using remote sensing and GIS—a case study of Nethravathi basin. Geosci Front 7(6):953–961

Gitas LZ, Douros K, Minakou C, Silleos GN, Karydas CG (2009) Multi-temporal soil erosion risk assessment in N. Chalkidiki using a modified USLE raster model. Earsel Eproceed 8(1):40–52

Gitelson AA, Kaufman YJ, Merzlyak MN (1996) Use of a green channel in remote sensing of global vegetation from EOS-MODIS. Remote Sens Environ 58(3):289–298

Hay LE, Wilby RL, Leavesley GH (2000) A comparison of Delta change and downscaled GCM scenarios for three mountainous basins in the United States. JAWRA J Am Water Resour Assoc 36(2):387–397

Hosseini M, João P, Pelayo KO, Ritsema C, Geissen V (2018) Developing generalized parameters for post-fire erosion risk assessment using the revised Morgan-Morgan-Finney model. Catena 165: 358–368

Hulme M, Hossell JE, Parry ML (1993) Future climate change and land use in the United Kingdom. Geogr J 159(2):131–147

Immerzeel WW, Van Beek LPH, Bierkens MFP (2010) Climate change will affect the Asian water towers. Science 328(5984):1382–1385

IGBP (1996) Predicting global change impacts on mountain hydrology and ecology: integrated catchment hydrology/altitudinal gradient studies

Jain SK, Kumar S, Varghese J (2001) Estimation of soil erosion for a Himalayan watershed using GIS technique. Water Resour Manag 15(1):41–54

Jiang L, Yao Z, Liu Z, Wu S, Wang R, Wang L (2015) Estimation of soil erosion in some sections of lower Jinsha River based on RUSLE. Nat Hazards 76(3):1831–1847

Jiao J, Xie Y, Lin Y, Zhao D (2009) Study on rainfall-runoff erosivity index in Northeastern China. Sci Soil Water Conserv 7(3):6–11 (In Chinese with English Abstract)

Khaleghpanah N, Shorafa M, Asadi H, Gorji M, Davari M (2016) Modeling soil loss at plot scale with EUROSEM and RUSLE2 at stony soils of Khamesan watershed, Iran. Catena 147:773–788

Laflen JM, Lane LJ, Foster GR (1991) WEPP: a new generation of erosion prediction technology. J Soil Water Conserv 46(1):34–38

Lal R (ed) (1998) Soil quality and soil erosion. CRC Press, Soil and Water Conservation Society, Boca Raton 329 pp

Lal R (2003) Soil erosion and the global carbon budget. Environ Int 29(4):437–450

Lei W, Wen Z (2008) Research on soil erosion vegetation factor index based on community structure. J Soil Water Conserv 22(5):68–72 (in Chinese)

Li ZY, Fang HY (2016) Impacts of climate change on water erosion: a review. Earth Sci Rev 163:94–117

Liu BY, Nearing MA, Shi PJ, Jia ZW (1994) Slope length effects on soil loss for steep slopes. Soil Sci Soc Am J 64(5):1759–1763

Liu BT, Tao HP, Shi Z, Song CF, Guo B (2014) Spatial distribution characteristics of soil erodibility K value in Qinghai-Tibet Plateau. Bull Soil Water Conserv 34:11–16 (in Chinese)

Lu XX, Ran LS, Liu S, Jiang T, Zhang SR, Wang JJ (2013) Sediment loads response to climate change: a preliminary study of eight large Chinese rivers. Int J Sediment Res 28(1):1–14

Ma T, Duan Z, Li R, Song X (2019) Enhancing SWAT with remotely sensed LAI for improved modelling of ecohydrological process in subtropics. J Hydrol 570:802–815

Mccool DK, Brown LC, Foster GR, Mutchler CK, Meyer LD (1987) Revised slope steepness factor for the universal soil loss equation. Trans ASAE - Am Soc Agric Eng (USA) 30(5):1387–1396

Meyer LD (1984) Evolution of the universal soil loss equation [erosion]. J Soil Water Conserv 39(2):99–104

Millward AA, Mersey JE (1999) Adapting the RUSLE to model soil erosion potential in a mountainous tropical watershed. Catena 38(2):109–129

Ministry of Water Resource of China (2008). SL190-2007 Standard for classification and gradation of soil erosion [S]. Beijing: China Water Conservancy and Hydropower Press: 3–12

Morgan RPC, Quinton JN, Smith RE, Govers G, Poesen J, Auerswald K et al (1998) The European Soil Erosion Model (EUROSEM): documentation and user guide

Morgan RPC, Morgan DDV, Finney HJ (1984) A predictive model for the assessment of soil erosion risk. J Agric Eng Res 30(3):245–253

Musa A, Liu Y, Wang A, Niu C (2016) Characteristics of soil freeze-thaw cycles and their effects on water enrichment in the rhizosphere. Geoderma 264:132–139

Naqvi HR, Mallick J, Devi LM, Siddiqui MA (2013) Multi-temporal annual soil loss risk mapping employing revised universal soil loss equation (RUSLE) model in Nun Nadi watershed, Uttrakhand (India). Arab J Geosci 6(10):4045–4056

Nearing MA, Foster GR, Lane LJ, Finkner SC (1989) A process-based soil erosion model for USDA-water erosion prediction project technology. Trans ASAE 32(5):1587–1593

Nearing MA, Lane LJ, Alberts EE, Laflen JM (1990) Prediction technology for soil erosion by water: status and research needs. Soil Sci Soc Am J 54(6):1702–1711

Nearing MA, Pruski FF, O'Neal MR (2004) Expected climate change impacts on soil erosion rates: a review. J Soil Water Conserv 59(1):43–50

Nearing MA, Jetten V, Baffaut C, Cerdan O, Couturier A, Hernandez M et al (2005) Modeling response of soil erosion and runoff to changes in precipitation and cover. Catena 61(2):131–154

Neitsch SL, Arnold IG, Kiniry IR, Williams IR (2009) Soil and Water Assessment Tool Theoretical Documentation Version 2009

Onori F, Bonis PD, Grauso S (2006) Soil erosion prediction at the basin scale using the revised universal soil loss equation (RUSLE) in a catchment of Sicily (southern Italy). Environ Geol 50(8):1129–1140

Ozsoy G, Aksoy E, Dirim MS, Tumsavas Z (2012) Determination of soil erosion risk in the Mustafakemalpasa River basin, Turkey, using the revised universal soil loss equation, geographic information system, and remote sensing. Environ Manag 50(4):679–694

Parajuli PB, Jayakody P, Sassenrath GF, Ouyang Y (2016) Assessing the impacts of climate change and tillage practices on stream flow, crop and sediment yields from the Mississippi River Basin. Agric Water Manag 168:112–124

Park S, Oh C, Jeon S, Jung H, Choi C (2011) Soil erosion risk in Korean watersheds, assessed using the revised universal soil loss equation. J Hydrol 399(3-4):263–273

Porto P, Walling DE, Callegari G (2011) Using 137Cs measurements to establish catchment sediment budgets and explore scale effects. Hydrol Process 25:886–900

Pruski FF, Nearing MA (2002) Runoff and soil-loss responses to changes in precipitation: a computer simulation study. J Soil Water Conserv 57(1):7–15

PSIAC (1968) Pacific Southwest Inter-Agency Committee. Report of the Water Management Sub-Committee. Sedimentation Task Force. 10. ASCE. 98. Report HY12

Renard KG, Foster GR, Weesies GA (1997) Predicting soil erosion by water: a guide to conservation planning with the revised universal soil loss equation (RUSLE). Agriculture Handbook No. 703. US Department of Agriculture, Washington D.C.

Renard K, Yoder D, Lightle D, Dabney S (2011) Universal soil loss equation and revised universal soil loss equation. Handbook of erosion modelling. Blackwell Publishing, Oxford, pp 137–167

Renschler CS, Mannaerts C, Diekkrüger B (1999) Evaluating spatial and temporal variability in soil erosion risk—rainfall erosivity and soil loss ratios in Andalusia, Spain. Catena 34(3-4):209–225

Routschek A, Schmidt J, Kreienkamp F (2014) Impact of climate change on soil erosion—a high-resolution projection on catchment scale until 2100 in Saxony/Germany. Catena 121:99–109

Sahin U, Angin I, Kiziloglu FM (2008) Effect of freezing and thawing processes on some physical properties of saline–sodic soils mixed with sewage sludge or fly ash. Soil Tillage Res 99(2):254–260

Schmidt S, Alewell C, Meusburger K (2018) Mapping spatio-temporal dynamics of the cover and management factor (C-factor) for grasslands in Switzerland. Remote Sens Environ 211:89–104

Serpa D, Nunes JP, Santos J, Sampaio E, Jacinto R, Veiga S, Lima JC, Moreira M, Corte-Real J, Keizer JJ, Abrantes N (2015) Impacts of climate and land use changes on the hydrological and erosion processes of two contrasting Mediterranean catchments. Sci Total Environ 538:64–77

Sharpley AN, Williams JR (1990) EPIC–Erosion/Productivity Impact Calculator: 1. Model documentation. USDA Technical Bulletin No. 1768, Washington, DC

Shi X, Zhang F, Lu X, Wang Z, Gong T, Wang G, Zhang H (2018) Spatiotemporal variations of suspended sediment transport in the upstream and midstream of the Yarlung Tsangpo River (the upper Brahmaputra), China. Earth Surf Process Landf 43(2)

Shinde V, Tiwari KN, Singh M (2010) Prioritization of micro watersheds on the basis of soil erosion hazard using remote sensing and geographic information system. Int J Water Resour Environ Eng 2(3): 130–136

SWCS (2003) Conservation implications of climate change: soil erosion and runoff from cropland

Tang JL, Cheng XQ, Zhu B, Gao MR, Wang T, Zhang XF, Zhao P, You X (2015) Rainfall and tillage impacts on soil erosion of sloping cropland with subtropical monsoon climate—a case study in hilly purple soil area, China. J Mt Sci 12(1):134–144

Tanyaş H, Kolat C, Süzen M (2015) A new approach to estimate cover-management factor of RUSLE and validation of RUSLE model in the watershed of Kartalkaya Dam. J Hydrol 528:584–598

Teng H, Liang Z, Chen S, Liu Y, Raphael A, Adrian C, Wu Y, Zhou S (2018) Current and future assessments of soil erosion by water on the Tibetan Plateau based on RUSLE and CMIP5 climate models. Sci Total Environ 635:673–686

Toy TJ, Foster GR, Renard KG (2002) Soil erosion: processes, prediction, measurement and control. Wiley, New York (338 pp)

USDA-Agricultural Research Service Washington D.C. (2008) Revised universal soil loss equation version 2

Van Leeuwen WJD, Sammons G (2004) Vegetation dynamics and erosion modeling using remotely sensed data (MODIS) and GIS. Tenth Biennial USDA Forest Service Remote Sensing Applications Conference, Salt Lake City, 5–9

Van der Knijff J, Jones R, Montanarella L (2000) Soil erosion risk assessment in Europe. European Soil Bureau, European Commission

Vente JD, Poesen J (2005) Predicting soil erosion and sediment yield at the basin scale: scale issues and semi-quantitative models. Earth Sci Rev 71:95–125

Vieira DCS, Serpa D, Nunes JPC, Prats SA, Neves R, Keizer JJ (2018) Predicting the effectiveness of different mulching techniques in reducing post-fire runoff and erosion at plot scale with the RUSLE, MMF and PESERA models. Environ Res 165:365–378

Wang G, Gertner G, Fang S, Anderson AB (2003) Mapping multiple variables for watershed using GIS technique. Water Resour Manag 15(1):41–54

Wang S, Fu B, Piao S, Lü Y, Ciais P, Feng X et al (2015) Reduced sediment transport in the yellow river due to anthropogenic changes. Nat Geosci 9(1):38–41

Wang YS, Cheng CC, Xie Y, Liu BY, Yin SQ, Liu YN et al (2017) Increasing trends in rainfall-runoff erosivity in the Source Region of the Three Rivers, 1961–2012. Sci Total Environ 592:639–648

Wischmeier WH, Smith DD (1978) Predicting rainfall erosion losses—a guide to conservation planning. Agriculture Handbook No. 537. US Department of Agriculture, Washington, D. C.

Wu CG, Li S, Ren HD, Yao XH, Huang ZJ (2012) Quantitative estimation of vegetation cover and management factor in USLE and RUSLE models by using remote sensing data: a review. Chin J Appl Ecol 23(6):1728–1732

Wu YY, Ouyang W, Hao ZC, Lin CY, Liu HB, Wang YD (2018) Assessment of soil erosion characteristics in response to temperature and precipitation in a freeze-thaw watershed. Geoderma 328:56–65

Xu L, Xu X, Meng X (2013) Risk assessment of soil erosion in different rainfall scenarios by RUSLE model coupled with information diffusion model: a case study of Bohai Rim, China. Catena 100(2):74–82

Xu YQ, Shao XM, Peng J (2009) Assessment of soil erosion using RUSLE and GIS: a case study of the Maotiao River watershed, Guizhou Province, China. Environ Geol 56:1643–1652

Yoder D, Lown J (1995) The future of RUSLE: inside the new revised universal soil loss equation. (Special issue: water research and management in semiarid environments). J Soil Water Conserv 50(5): 484–489

Zhang W, Fu J (2003) Rainfall erosivity estimation under different rainfall amount. Resour Sci 25:35–41 (In Chinese with English Abstract)

Zhang W, Xie Y, Liu B (2002) Rainfall erosivity estimation using daily rainfall amounts. Sci Geogr Sin 22:705–711 (In Chinese with English Abstract)

Zhang W, Huang B (2015) Soil erosion evaluation in a rapidly urbanizing city (Shenzhen, China) and implementation of spatial land-use optimization. Environ Sci Pollut Res 22:4475–4490. https://doi.org/10.1007/s11356-014-3454-y

Zhang XC, Nearing MA (2005) Impact of climate change on soil erosion, runoff, and wheat productivity in central Oklahoma. Catena 61(2-3): 185–195

Zhang XC (2007) A comparison of explicit and implicit spatial downscaling of GCM output for soil erosion and crop production assessments. Clim Chang 84(3-4):337–363

Zhang XC, Liu WZ, Li Z, Zheng FL (2009) Simulating site-specific impacts of climate change on soil erosion and surface hydrology in southern Loess Plateau of China. Catena 79(3):237–242

Zhang X, Wu S, Cao W, Guan J, Wang Z (2015) Dependence of the sediment delivery ratio on scale and its fractal characteristics. Int J Sediment Res 30(4):338–343

Zheng D (2003) Formation and development of the Qinghai-Tibet Plateau. Hebei Science and Technology Press (in Chinese)

Zhou P, Luukkanen O, Tokola T, Nieminen J (2008) Effect of vegetation cover on soil erosion in a mountainous watershed. Catena 75(3): 319–325

Zhou Z, Ma W, Zhang S, Mu Y, Li G (2017) Effect of freeze-thaw cycles in mechanical behaviors of frozen loess. Cold Reg Sci Technol 146: 9–18